

## Update: Cardiac Imaging (VI)

## Multidetector Computed Tomography for Congenital Anomalies of the Aortic Arch: Vascular Rings

Luis García-Guereta,<sup>a,\*</sup> Estefanía García-Cerro,<sup>a</sup> and Montserrat Bret-Zurita<sup>b</sup><sup>a</sup>Servicio de Cardiología Pediátrica, Hospital Universitario La Paz, Madrid, Spain<sup>b</sup>Servicio de Radiodiagnóstico, Radiología Pediátrica, Imagen Cardíaca Pediátrica y Cardiopatías Congénitas, Hospital Universitario La Paz, Madrid, Spain

## ABSTRACT

The development of multidetector computed tomography has triggered a revolution in the study of the aorta and other large vessels and has replaced angiography in the diagnosis of congenital anomalies of the aortic arch, particularly vascular rings. The major advantage of multidetector computed tomography is that it permits clear 3-dimensional assessment of not only vascular structures, but also airway and esophageal compression. The current update aims to summarize the embryonic development of the aortic arch and the developmental anomalies leading to vascular ring formation and to discuss the current diagnostic and therapeutic role of multidetector computed tomography in this field.

© 2016 Sociedad Española de Cardiología. Published by Elsevier España, S.L.U. All rights reserved.

## Keywords:

Vascular rings  
Aberrant subclavian artery  
Slings

## Tomografía computarizada con multidetectores en las anomalías congénitas del arco aórtico: anillos vasculares

## RESUMEN

El desarrollo de la tomografía computarizada con multidetectores ha supuesto una revolución en el estudio de la aorta y los grandes vasos y ha sustituido a la angiografía para diagnosticar las anomalías congénitas del arco aórtico, en particular los anillos vasculares. La tomografía computarizada con multidetectores ofrece la gran ventaja de que se puede evaluar nítidamente y en tres dimensiones no solo las estructuras vasculares, sino también la compresión en la vía aérea y el esófago. Queremos hacer un abordaje del desarrollo embriológico del arco aórtico y de las anomalías en su desarrollo que determinan la formación de anillos vasculares y ofrecer un enfoque actual del papel de la tomografía computarizada con multidetectores para su abordaje diagnóstico y terapéutico.

© 2016 Sociedad Española de Cardiología. Publicado por Elsevier España, S.L.U. Todos los derechos reservados.

## Palabras clave:

Anillos vasculares  
Subclavia anómala  
Slings

## INTRODUCTION

Vascular rings (VR) are congenital developmental abnormalities of the aortic arch consisting of vascular structures that encircle and sometimes compress the airway and esophagus.<sup>1</sup> The term VR was introduced by Robert Gross in 1948.<sup>2</sup> The rings can be complete, if the vascular structures fully encircle the airway and esophagus, or incomplete, known in the literature as slings, if the compression is incomplete (Table).<sup>1</sup> The most frequent congenital malformations of the aortic arch—specifically, left aortic arch with aberrant right subclavian artery (ARSA) and right arch with mirror-image branching—only form rings in exceptional situations.

The exact prevalence of VR is unclear because most data have been derived from historical series that collected data on symptomatic patients. However, these structures are currently often diagnosed in the prenatal period and are asymptomatic in

both the neonatal period and later years.<sup>3–6</sup> The most frequent VR are the double aortic arch (DAA) and the right arch with aberrant left subclavian artery (ALSA). In the DAA, the left and right aortic arches themselves compress the airway and esophagus. In the right aortic arch (RAA) with aberrant subclavian artery (RAA with ALSA), the compression is due to a retroesophageal course of the left subclavian artery and to a ligament resulting from closure of the left ductus arteriosus attaching the descending aorta (posterior) to the pulmonary artery (anterior).

Congenital heart disease detection has improved in recent decades due to greater diagnostic accuracy in the prenatal and neonatal periods. The prevalences of the various heart diseases are changing due to several factors, such as voluntary pregnancy interruption and a higher number of pregnancies in older women due to *in vitro* fertilization. Nonetheless, a recent study<sup>7</sup> showed a congenital heart disease prevalence of 67.7:10 000 live births, similar to that of classical epidemiological studies,<sup>8</sup> and reported a VR prevalence of 1:10 000 live births.<sup>7</sup> However, current fetal series report a VR incidence of 1 to 1.5:1000.<sup>3–6</sup> The conflicting

\* Corresponding author: Servicio de Cardiología Infantil, P.º de la Castellana 261, 28046 Madrid, Spain.

E-mail address: [luisguereta@gmail.com](mailto:luisguereta@gmail.com) (L. García-Guereta).

### Abbreviations

ALSA: aberrant left subclavian artery  
 ARSA: aberrant right subclavian artery  
 DAA: double aortic arch  
 KD: Kommerell diverticulum  
 MDCT: multidetector computed tomography  
 MRI: magnetic resonance imaging  
 RAA: right aortic arch  
 VR: vascular ring

figures suggest the presence of a wider disease spectrum, from mild prenatally detected cases with a practically asymptomatic clinical course<sup>4–6</sup> to serious situations from birth with severe breathing difficulty due to tracheal problems.<sup>3–6</sup>

The respiratory symptoms are secondary to compression of the airway and can first manifest as severe respiratory distress syndrome or marked inspiratory stridor. Less marked symptoms can also be evident, such as bronchospasm or recurrent respiratory infections. The symptoms of esophageal compression consist of alterations in the swallowing of solids or liquids and are more frequent in older patients, whereas respiratory symptoms are predominant in infants.<sup>9–11</sup>

The techniques traditionally used for the diagnosis of these anomalies have been esophagography, echocardiography, and angiography. Tracheoesophageal compression is both from left to right and anterior to posterior for a DAA, whereas it is fundamentally posterior if there is an aberrant left or right subclavian artery. The compression zones can be visualized using barium esophagography. Anterior esophageal compression is characteristic of pulmonary artery slings because the left pulmonary artery passes between the trachea and esophagus.<sup>9–11</sup> Although echocardiography is systematically performed, it is not the most useful technique because of its high false-negative rate, particularly for an aberrant left or right subclavian artery. The typical arrangement of the large vessels in a RAA mirrors that of the left aortic arch, so that the first vessel is the left brachiocephalic trunk. The clue for ultrasound diagnosis of an aberrant left or right subclavian artery is the absence of a bifurcation of the first supraaortic trunk, but imaging of this structure is difficult, even in selected patients prenatally diagnosed with a VR.<sup>11,12</sup> Angiography is usually performed to confirm diagnosis but has been relegated to the past by the noninvasive diagnostic capability of magnetic resonance imaging (MRI) and computed tomography.<sup>13–15</sup> Bronchoscopy can be used to dynamically check for tracheal compression, as well as to rule out intrinsic disease of the airway. Multidetector computed tomography (MDCT) not only permits diagnosis of aberrant vessels, but provides clear images of the

**Table**  
Types of Vascular Rings

Complete vascular rings	Incomplete vascular rings
Double aortic arch	LAA + ARSA
RAA with mirror-image branching and posterior ligament	RAA with mirror-image branching
RAA with ALSA and left PDA	RAA with isolated LSA
RAA with isolated LSA and right PDA	Pulmonary sling
Descending aorta contralateral to the aortic arch and contralateral PDA	

ALSA, aberrant left subclavian artery; ARSA, aberrant right subclavian artery; LAA, left aortic arch; LSA, left subclavian artery; PDA, patent ductus arteriosus; RAA, right aortic arch.

airway, as well as virtual reconstruction of the tracheobronchial tree, enabling the selection of patients for preoperative bronchoscopy.<sup>13–15</sup>

The latest technique to be added to the VR diagnosis arsenal is fetal echocardiography. Incorporation of the 3-vessel and tracheal views<sup>16</sup> and their widespread use in routine fetal heart screening has facilitated the diagnosis of aortic arch anomalies in the fetal stage.<sup>3–6,9–12</sup> The presence of RAA should suggest a possible VR, particularly if ALSA is also present. The various prenatal diagnosis techniques have achieved a high degree of diagnostic accuracy.<sup>3–6,9–12,17–19</sup>

### MULTIDETECTOR COMPUTED TOMOGRAPHY

The image acquisition process of MDCT involves constant table movement while the gantry continually rotates and emits X-rays. The attenuation of the X-rays varies according to the density of the different tissues and is received by X-ray detectors. In the final image, consisting of an attenuation map, each pixel has a value reflecting the composition of each tissue.<sup>20</sup> Because the damage caused by X-rays is directly related to age, the radiosensitivity of growing organs, and the effect of the radiation accumulation until adulthood, there is a stronger cause-effect relationship in children.<sup>20–22</sup> The aim is always to achieve the maximum diagnostic benefit with the lowest possible radiation dose.<sup>15,20–22</sup> In pediatric congenital heart disease studies, monomeric low-osmolarity nonionic contrast agent at 300 mg/mL is used at a dose of 1.5–2.0 mL/kg body weight.<sup>15,23</sup> The agent should be introduced with a dual-head automatic injector, with an injection velocity depending on the canalized vessel.

A single spiral image is typically obtained of the region from the thoracic lid to the dome of the diaphragm, and acquisition begins with automatic tracking of the bolus in the aorta. The reconstructed volume is sent to the auxiliary console, equipped with various predefined reconstruction algorithms and techniques: aortic or cardiac, multiplanar, maximum intensity projection and 3-dimensional (3D) volumetry for vascular and multiplanar structures, and surface rendering or virtual navigation to evaluate the airway.<sup>15</sup>

### DEVELOPMENT OF THE AORTIC ARCH ANOMALIES. EMBRYOLOGY

Vascular rings are secondary to alterations in embryonic development occurring between the third and eighth weeks of gestation, during the development of the thoracic aorta and the main arterial trunks. Initially, the embryonic vascular network is formed by 2 central vessels, the dorsal aorta and primitive ventral aorta, connected to each other via 6 pairs of arches and intersegmental arteries. Involution occurs of most of the first, second, and fifth arches. The third aortic arches give rise to the carotid artery. The ventral portion of the sixth arches gives rise to the proximal pulmonary arteries. On the left side, the dorsal contribution of the sixth arch gives rise to the ductus arteriosus. The intersegmental arteries originate from the dorsal aorta and form the subclavian arteries (Figure 1A).<sup>9,24</sup>

Edwards proposed a hypothetical model of the DAA in 1948 (Figure 1B).<sup>25</sup> The model shows an aortic arch and a ductus arteriosus on each side with the dorsal aorta in the center. The left and right supra-aortic trunks develop from the left and right aortic arches, respectively. The carotid arteries are anterior and the subclavian arteries are posterior. This model helps to explain both normal development and potential abnormalities, which depend on the location of the system interruption. It is still unknown why a

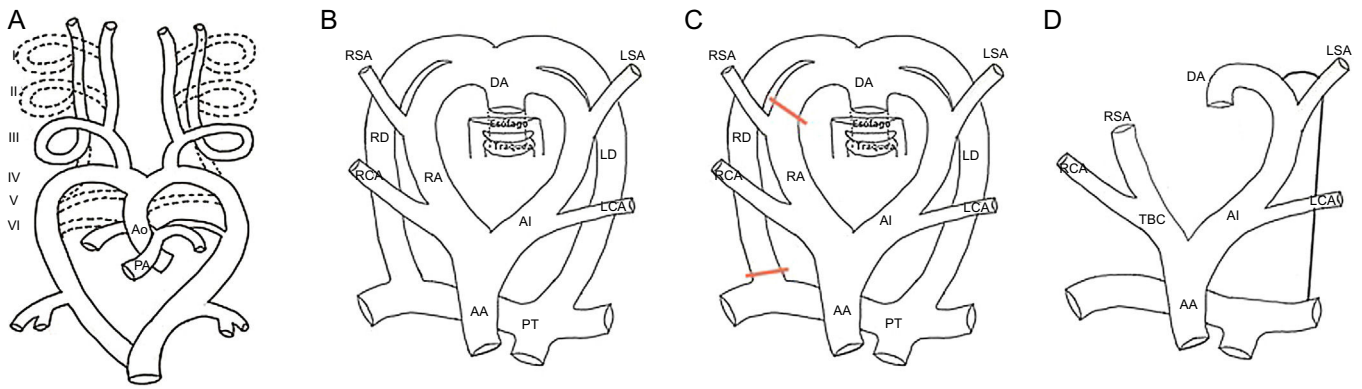


**Figure 1.** A: Drawing of the embryonic branchial arches. B: Hypothetical model of Edwards. C: Normal regression (left aortic arch). D: Drawing of the left aortic arch. AA, ascending aorta; DA, descending aorta; LCA, left carotid artery; LD, left ductus; LSA, left subclavian artery; PT, pulmonary trunk; RA, right arch; RCA, right carotid artery; RD, right ductus; RSA, right subclavian artery; BCT, brachiocephalic trunk.

left arch develops during embryogenesis and not a right arch<sup>26</sup> but the arch is normally left in humans and is formed by regression of the dorsal segment of the right arch, between the right subclavian

artery and the descending aorta and the right ductus arteriosus (Figure 1C). The trachea remains behind and to the right of the arch and the left ductal ligament is in front and to the left of the arch

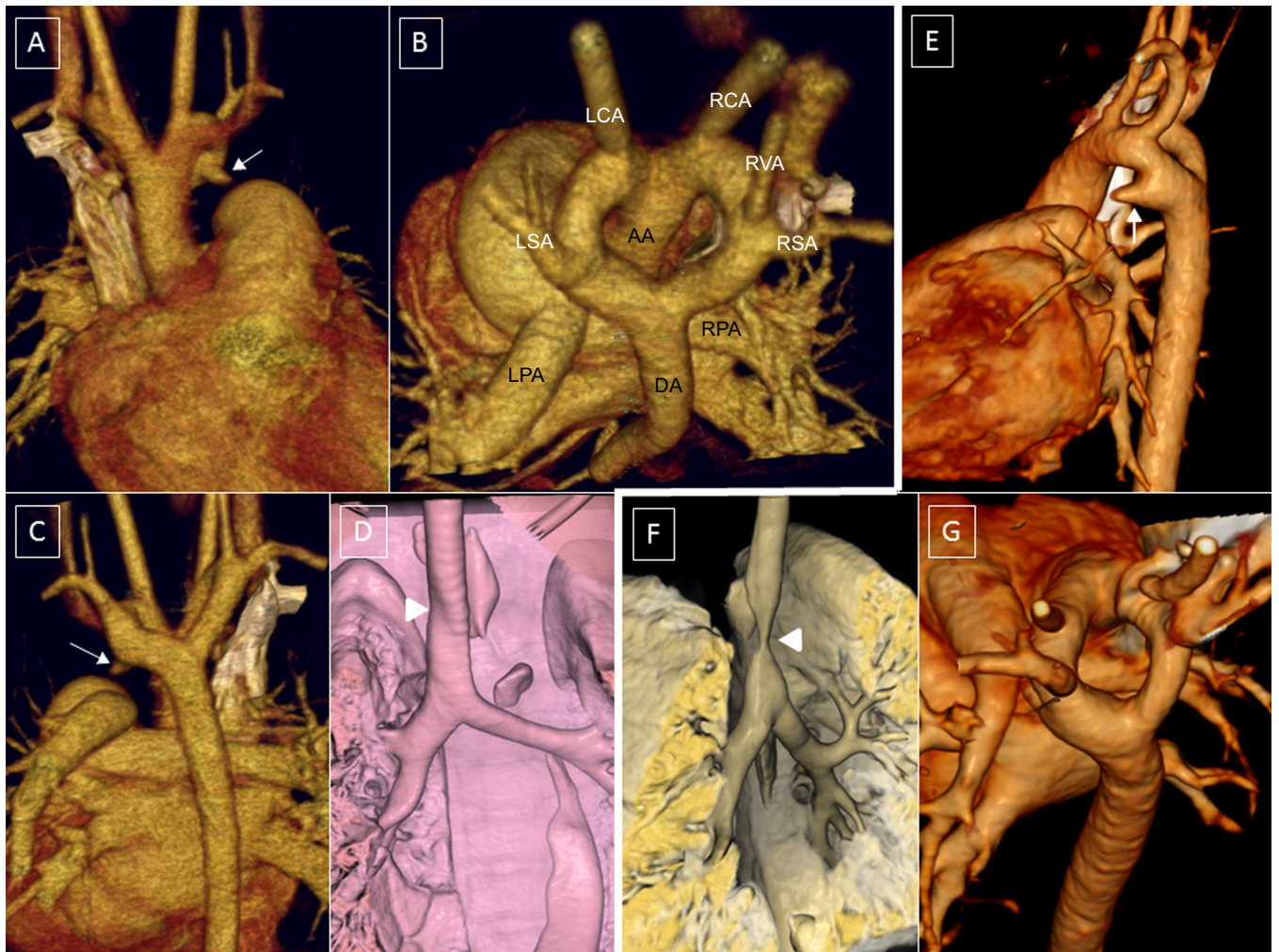


**Figure 2.** A-D (case 1): Computed tomography coronary angiography with 3-dimensional volumetric reconstruction; 4-year-old patient with Rubinstein-Taybi syndrome with suspected double aortic arch, interventricular communication, and ductus arteriosus. A: Anterior view, right ascending aorta, double arch; small ductal ampulla of the left aortic arch (arrow). B: Posterosuperior view, wide double aortic arch. C: Posterior view, right descending aorta, with slight elevation of the right arch with respect to the left arch and a slightly smaller caliber. D: Reconstruction of the main airway; minor impact on the airway (arrowhead). E and F (case 2): 9-day-old patient. E: Left lateral view; left ductal ampulla (arrow). F: Trachea, right lateral view; the aortic double arch produces a critical tracheal stenosis (arrowhead). G: Posterosuperior view; the caliber of the left arch is slightly larger than that of the right. AA, ascending aorta; DA, descending aorta; LCA, left carotid artery; LPA, left pulmonary artery; LSA, left subclavian artery; RCA, right carotid artery; RPA, right pulmonary artery; RSA, right subclavian artery; RVA, right vertebral artery.

(Figure 1D). When the interruption occurs at another level, it gives rise to a different vascular conformation that can produce a VR or vascular sling.

## TYPES OF VASCULAR RINGS

### Double Aortic Arch

The DAA is the easiest ring to understand. It is simply explained by the persistence of the embryonic system of Edwards (Figure 1B). The ascending aorta is divided into 2 arches, right and left, which encircle the trachea and esophagus and connect behind the esophagus to form the descending aorta. Each arch independently gives rise to the carotid arteries in front and the subclavian arteries behind. The left ductus usually persists, becoming a ligament upon closure. Persistence of the right ductus or both ducti is rare<sup>9</sup> (Figure 2).

The 2 arches can be of a similar caliber or 1 can predominate, typically the right. Regression can also occur of a vascular segment, becoming a ligamentous structure. Such regression is more common for the posterior arches, understood to be those between the subclavian artery and the descending aorta (Figure 3). When the left posterior arch completely regresses (Figure 3A and B), it is difficult to distinguish the anomaly from a RAA with normally associated vessels. In this case, there would be a common origin of

the carotid and left subclavian arteries in a common trunk (left brachiocephalic artery) (Figure 4B and Figure 5),

Multidetector computed tomography provides a highly accurate diagnostic view. The cranial view is the most realistic view of the vascular structures of the ring and their compression.<sup>27</sup> The smaller the space inside the ring, the earlier the onset and the more severe the symptoms (Figure 2). Three-dimensional reconstruction images are very useful for surgical planning; the ideal surgical approach involves division of the smallest arch between the subclavian artery and the descending aorta. Although most patients require surgery, the area enclosed by the ring is sometimes large, delaying symptom onset and deferring or even obviating the need for surgery. Close clinical follow-up is required because there have been reports of sudden death from severe respiratory disease.<sup>28</sup>

### Right Aortic Arch

The RAA is the most common aortic arch anomaly. It is caused by regression of the junction of the embryonic left arch and the descending aorta (Figure 4). Its estimated incidence is between 0.086% and 0.1% of pregnancies in populations with a low risk of congenital heart disease.<sup>3–6,12,17–19,29</sup> It is usually accompanied by intracardiac malformations, mainly tetralogy of Fallot and pulmonary atresia. Often, the RAA is associated with chromosomal

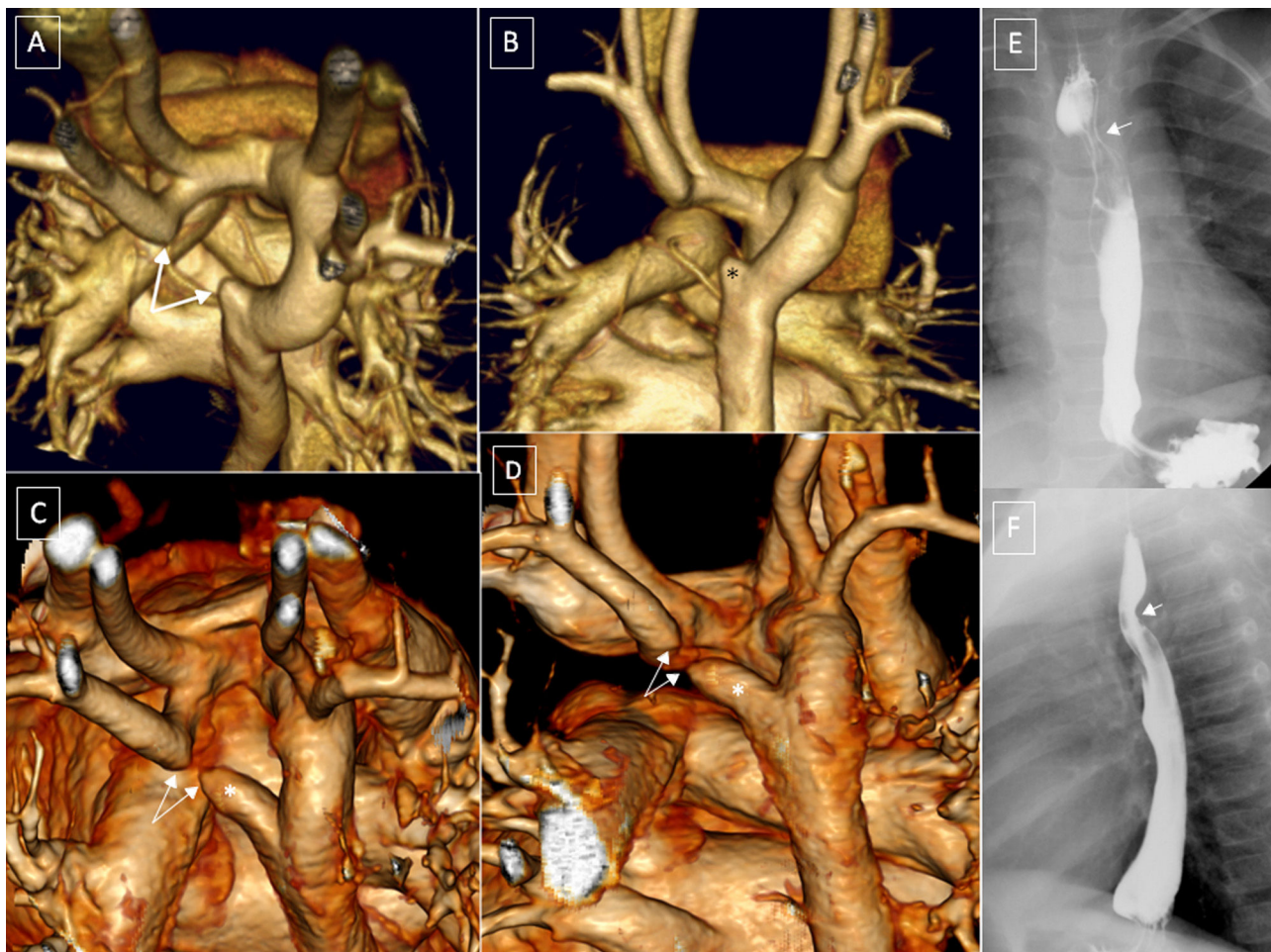


**Figure 3.** Computed tomography coronary angiography, 3-dimensional volumetric reconstruction. A and C: Posterosuperior view; deformities due to the possible presence of a ligament in the left arch that closes the ring (arrows). B and D: Posterior view of the aortic arch with different degrees of regression of the left posterior arch (\*). E and F: esophagography showing secondary compression (small arrows).

anomalies or extracardiac alterations, but it can also present in isolation or with mild anomalies.<sup>17–19</sup>

#### Right Aortic Arch With Mirror-image Branching, Edwards Type I

This is the most frequent type of RAA. The left anterior arch forms the right brachiocephalic trunk, which is anterior. The embryonic right arch persists and forms a RAA, and the left ductus becomes a ligament that remains anterior and does not normally form a ring (Figure 4B).

Fetal series have shown its almost constant association with complex intracardiac malformations and chromosomal anomalies, particularly 22q11 deletion.<sup>3–6</sup> Although RAA with mirror-image branching does not usually form a ring (Figure 4B), it can on rare occasions form a VR when there is a persistent ductus<sup>9,26,29</sup> connecting the right descending aorta with the pulmonary artery (Figure 4D and Figure 5). The ductus would pass behind the esophagus and run forward to connect with the pulmonary artery, which is anterior. After birth, upon closure of the ductus, the ductal ligament would close the VR and divert the trachea to the left, compressing it (Figure 5).

In these situations, the posterior compression is not due to a vascular structure, but to the ligament itself. Accordingly, no vascular structure can be seen using MDCT (Figure 5). The embryonic hypothesis would imply a regression of the left posterior arch proximal to the attachment of the ductus (Figure 4A and C).

Such a diverticulum of the posterior aorta could contribute to ring formation (Figure 5). This formation is known as Kommerell diverticulum (KD), named after the physician who made the first nonpostmortem description of this structure in 1936.<sup>30</sup> His report involved a patient who presented with a left arch with ARSA. The ductal ligament arises from the KD. This ligament is not visible with MDCT because it lacks a vascular lumen but it can produce a deformity in both the KD and the pulmonary artery that reflects the attachment points of the ligament (Figure 4C and Figure 5B and E). There may even be a persistent ligament joining the descending aorta with the pulmonary artery without evidence of KD in some patients with RAA with mirror-image branching.<sup>26,29</sup>

#### Right Aortic Arch With Aberrant Left Subclavian Artery, Edwards Type II

The left subclavian artery forms as the last branch of the aortic arch, is posteriorly located, and runs behind the esophagus to the left arm.<sup>29</sup> The ring is completed by the ductal ligament, which joins the region of the descending aorta, where the left subclavian artery (posterior) arises, with the pulmonary artery (anterior) (Figure 4D and Figure 6). The junction of the left subclavian artery and the aorta normally remains dilated and forms a KD, whose presence indicates the existence of a ductal ligament at the apex of the aorta directed toward the left pulmonary artery.

In some patients with RAA with ALSA and tetralogy of Fallot, there might not be a KD and the structure is postulated to be due to

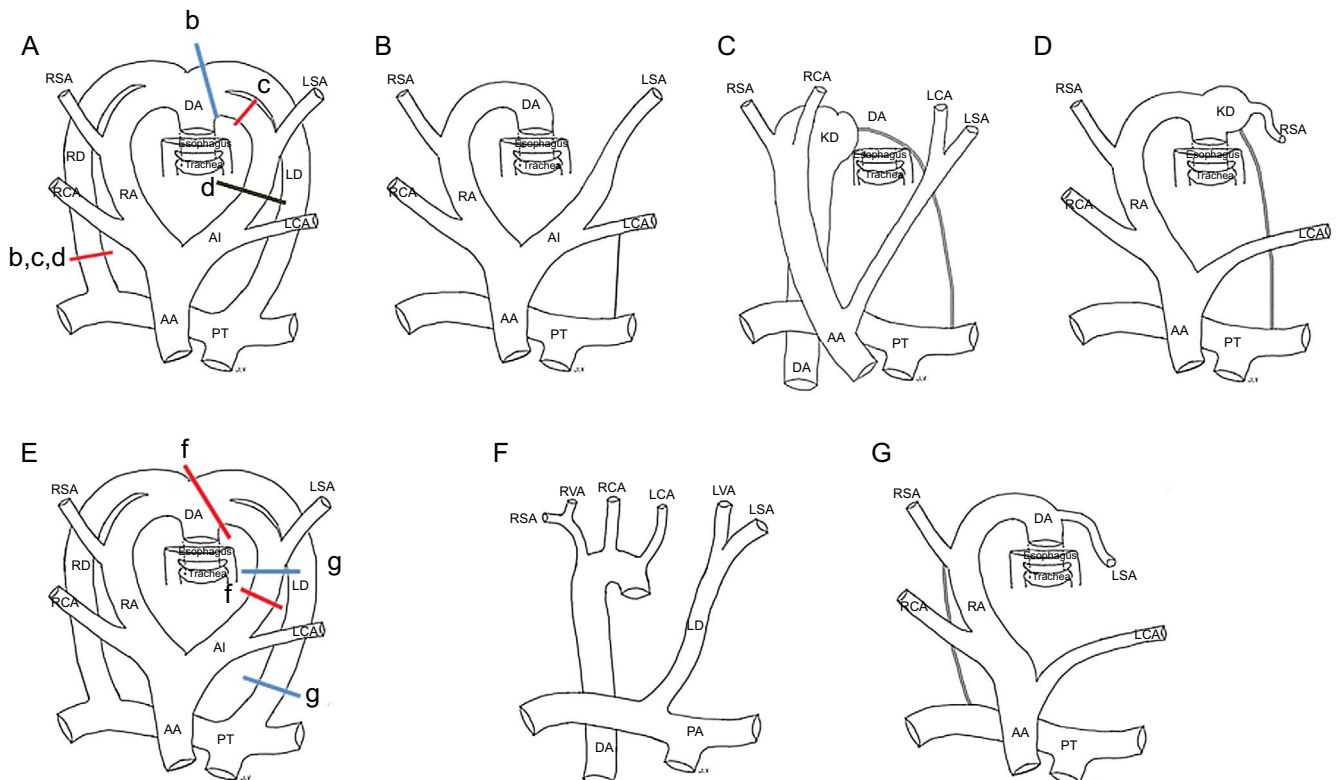


**Figure 4.** Embryonic development of the distinct types of right aortic arch. A and E: Hypothetical model; the regression of the segments of the left or right aortic arches and ducti from various points (lines b–d, f, and g in A and E) lead to the formation of the distinct types of the right aortic arch (B–D, F, and G); B: Right aortic arch with mirror-image branching and ductal ligament (without vascular ring); C: Right aortic arch with Kommerell diverticulum and vascular ring; D: Right aortic arch with Kommerell diverticulum and aberrant left subclavian artery; F: Right aortic arch with isolation of the left subclavian artery and connection of this vessel to the pulmonary artery; G: Right aortic arch with aberrant left subclavian artery and right ductus. AA, ascending aorta; DA, descending aorta; KD, Kommerell diverticulum; LCA, left carotid artery; LD, left ductus; LSA, left subclavian artery; LVA, left vertebral artery; PT, pulmonary trunk; RA, right arch; RCA, right carotid artery; RD, right ductus; RSA, right subclavian artery; RVA, right vertebral artery.

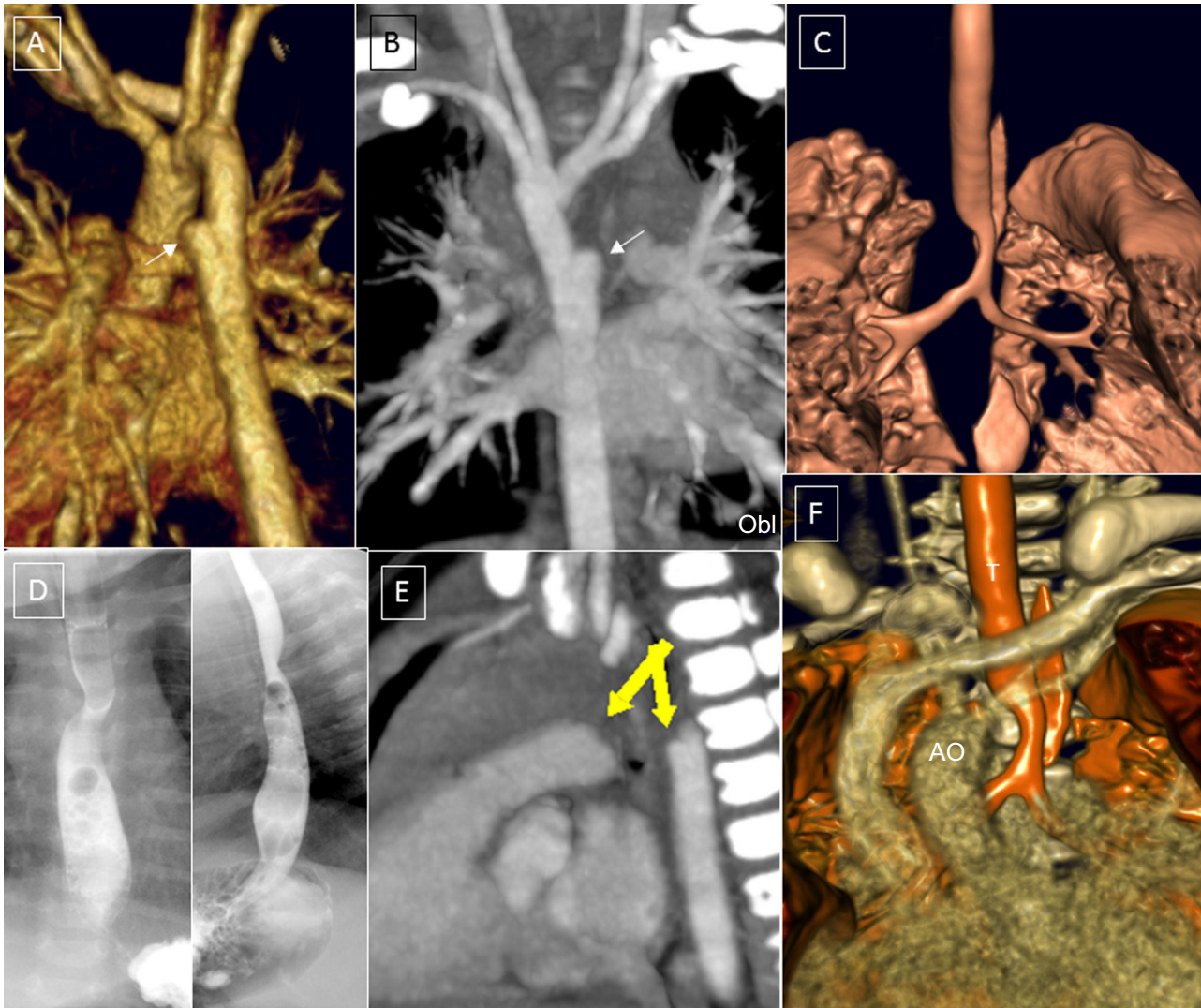


**Figure 5.** Right aortic arch with mirror-image branching. A and B: Small dilatation at the left edge of the descending aorta (arrow). C and F: 3-dimensional reconstruction of the airway with distal tracheobronchial compression indicated by the indent on the right aortic arch. D: posterior and lateral esophageal compression. E: Small excrescences suggested in the superior edge of the pulmonary artery and aorta, indicating a ductal ligament (yellow arrows). AO, aorta; T, trachea.

regression of the left ductus during gestation. Accordingly, there is no ductal ligament or diverticulum, and no VR.<sup>9</sup>

The resulting ring of an RAA with ALSA is not as tight as that produced by a DAA and is much less symptomatic. The severity of the resulting tracheal and esophageal compression largely depends on the dilatation of the KD. There are usually no symptoms in newborns and infants.

A recently presented multicenter Spanish series<sup>31</sup> studied 73 patients with a VR detected during pregnancy and showed, as in other fetal studies, that most patients with RAA with ALSA have no intracardiac malformations, in contrast to those with RAA with mirror-image branching.<sup>6,12,17,18</sup> This former defect is occasionally associated with chromosomal anomalies. The symptoms evident in infancy are predominantly respiratory,<sup>9–11</sup> whereas the predominant symptoms in adults involve dysphagia.<sup>32</sup> There have also been reports of aortic dissection<sup>33</sup> and aortic rupture<sup>34</sup> in adults.

Multidetector computed tomography (Figure 6) shows the position of the aortic arch to the right of the trachea and spine, indicates the presence of an ALSA, and can reveal the origin of the ductal ligament, from the KD in this case. The technique also shows the size of the ring and the degree of airway and esophageal compression.

Surgery is indicated for symptomatic patients and involves, at a minimum, resection of the ductal ligament via left thoracotomy.<sup>35,36</sup> Some groups have used thoracoscopy<sup>37</sup> for VR division, although this technique has also been reported to have a longer operative time with few benefits.<sup>38</sup> As well as ligament division, the diverticulum can be resected and aortopexy of the aortic arch can be performed to avoid reoperations.<sup>36–39</sup> Some authors<sup>40,41</sup> now recommend systematic diverticulum division and resection of the left subclavian artery and its reanastomosis to the left carotid artery because some patients in their series required reoperation due to KD dilatation.<sup>42</sup> Histological study after primary diverticulum resection can indicate cystic medial necrosis in up to 50% of patients, even in very young children,<sup>41</sup> a finding possibly related to later dilatation of the diverticulum, as described in adults.<sup>32–34</sup>

The approach to asymptomatic patients is controversial because the condition is usually diagnosed during pregnancy and affected individuals can remain asymptomatic in the long-term. Most centers perform some type of postnatal confirmatory test of the VR, particularly echocardiography, but MRI has been proposed due to the limitations of echocardiography. There is no agreement on the indication for MRI in newborns diagnosed with

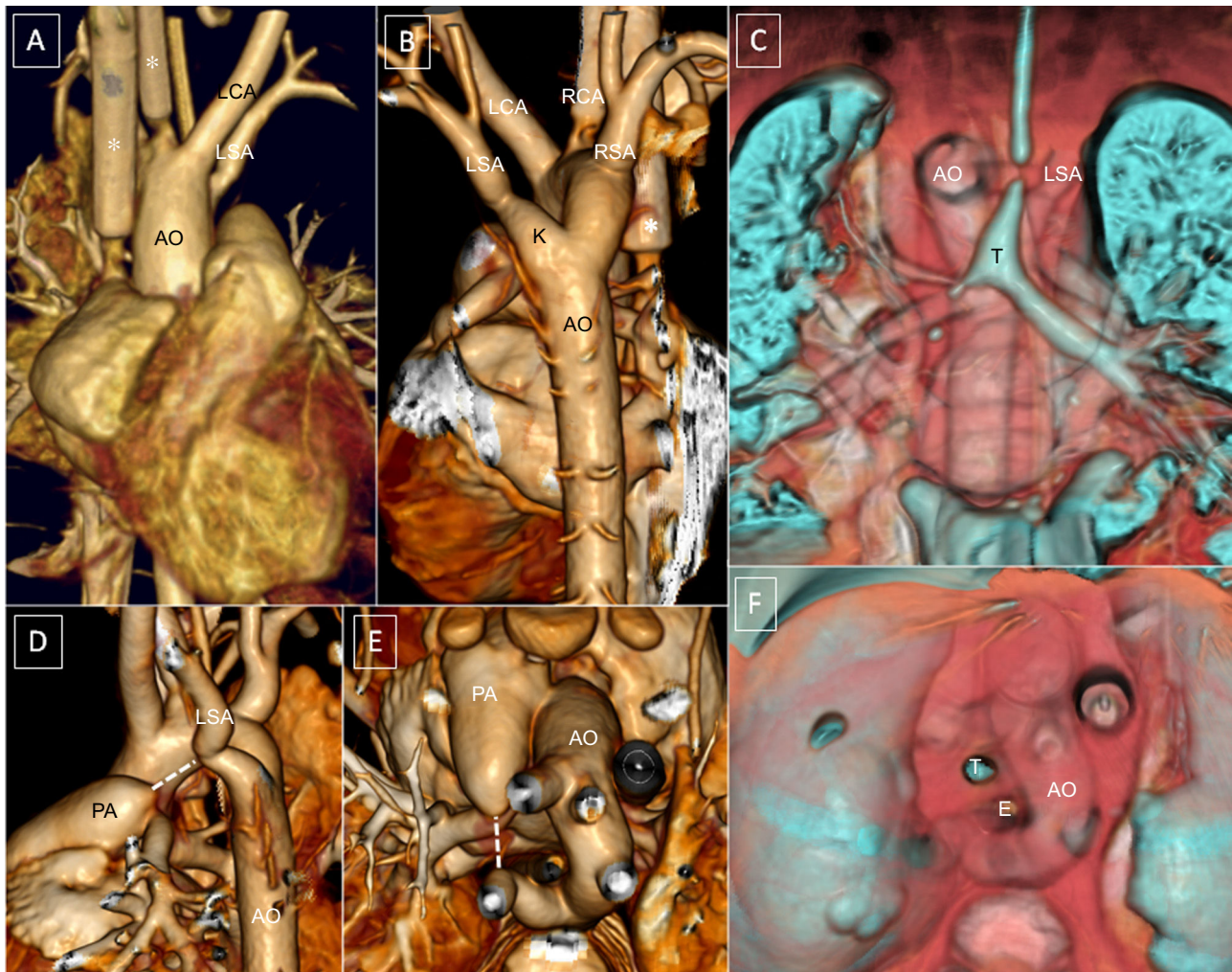


**Figure 6.** Right aortic arch (RAA) with aberrant left subclavian artery (ALSA); 20-day-old patient with tetralogy of Fallot, with extracorporeal membrane oxygenation cannulae. \*: arterial and venous cannulae. A and B: RAA with ALSA. C: Kommerell diverticulum and severe tracheal hypoplasia. D and E: Left and posterosuperior lateral view; excrescence of the superior edge of the pulmonary trunk and of the anterior edge of the left subclavian artery indicating ligament presence (dotted line). C and F: Coronal and posterosuperior reconstruction of the airway and vessels. AO, aorta; E, esophagus; K, Kommerell diverticulum; LCA, left carotid artery; LSA, left subclavian artery; PA, pulmonary artery; RCA, right carotid; RSA, right subclavian artery; T, trachea.

RAA with ALSA during the fetal stage. Magnetic resonance imaging has been proposed for symptomatic patients and those in whom the presence of VR cannot be confirmed by expert-performed echocardiography.<sup>6,43</sup> Additionally, MDCT with radiation-reducing techniques can be indicated.<sup>15,21,22</sup> Multi-detector computed tomography offers major advantages due to its better image quality and speed, as well as obviating the need for patient anesthesia and being widely available. In addition, MDCT shows the degree of airway involvement, thereby providing general information on the degree of compression and the possibility of unexpected complications in asymptomatic patients.

#### *Right Aortic Arch With Isolation of The Left Subclavian Artery, Edwards Type III*

This is the most infrequent of the RAAs. The left subclavian artery is isolated from the arch and connected to the ductus arteriosus. Its embryonic origin is due to interruption of the left arch of the Edwards model at 2 sites: between the carotid and left subclavian arteries and at the attachment of the left posterior arch<sup>9,44</sup> (Figure 4E and F). These changes interrupt the connection

between the aorta and the left subclavian artery, which remains connected to the pulmonary artery via the ductus (Figure 7).

This structure is usually associated with other cardiac malformations, mainly patent ductus arteriosus and aortic coarctation. The malformation is also associated with chromosomal anomalies, particularly 22q11 deletion. In these situations, cerebral steal syndrome can occur via the circle of Willis. After birth, the ductus can regress and the subclavian artery can become disconnected from the pulmonary artery (Figure 7C and D), which is why it is also known as isolated left subclavian artery. If the ductus remains patent (Figure 7A and B) and is not stenotic, it can be established as a descending channel from the left vertebral artery to the pulmonary artery. When the ductus is closed (Figure 7C and D), a channel has also to be established to the subclavian artery via the circle of Willis and the left vertebral artery.

An even more infrequent occurrence is isolation of the brachiocephalic trunk, which would correspond to an involution of the anterior segment of the left aortic arch, proximal to the origin of the left carotid artery in the Edwards model (Figure 7E and F). Color Doppler ultrasound of the neck vessels would show retrograde flow in the left carotid artery in these patients, because

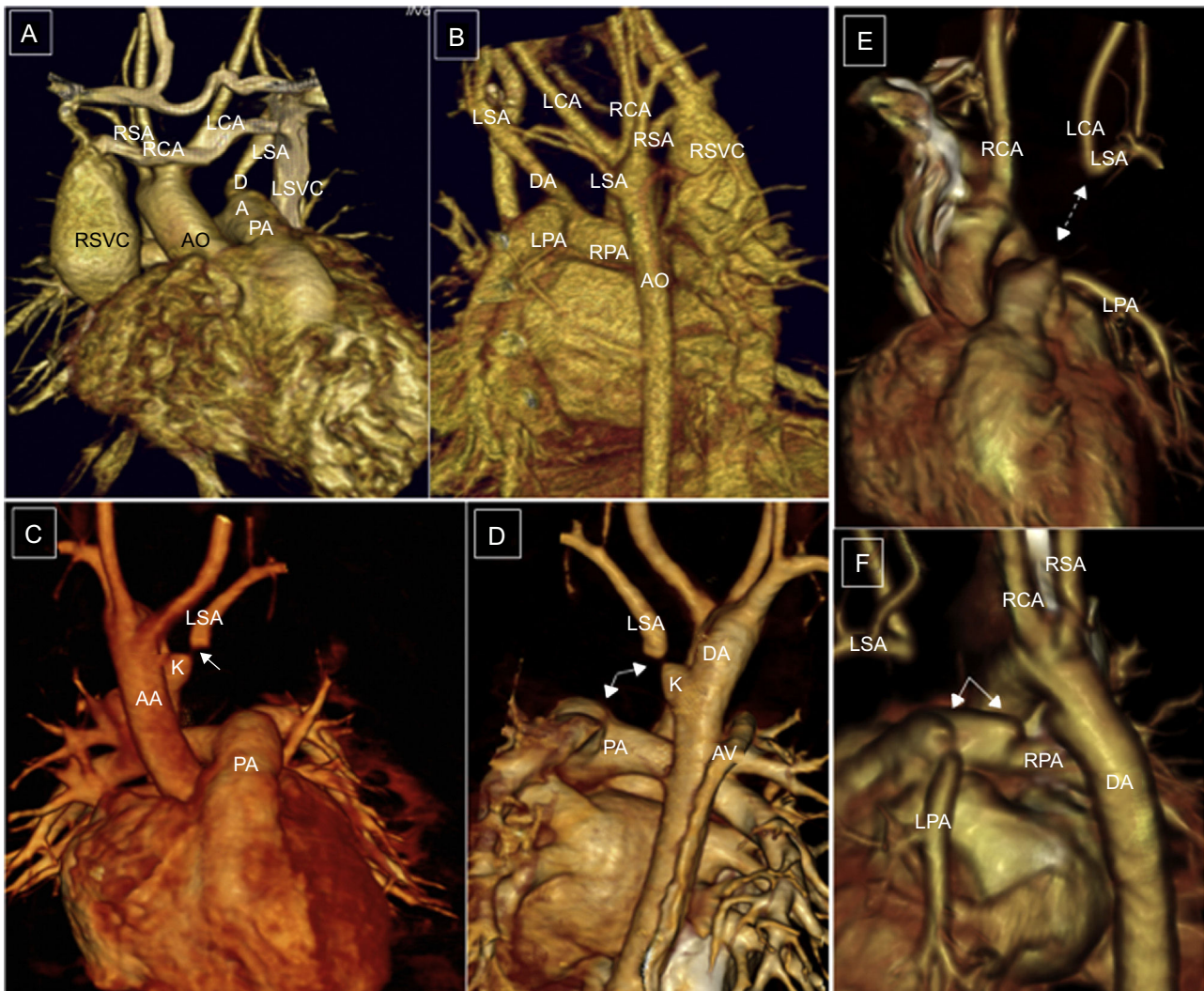


**Figure 7.** Right aortic arch with isolation of the left subclavian artery. A and B: Continuity of the distal left subclavian artery (LSA) with the ductus arteriosus. C and D: Anterior and posterior view, small Kommerell diverticulum and interruption of contrast agent flow (arrows). E and F: Isolation of the left brachiocephalic trunk. E: Anterior view, hypothetical ductus arteriosus (arrow, dots). F: left lateral view, right aortic arch, ductal ampulla, and ductal ligament; small diverticula indicating the presence of ligaments (arrows). AO, aorta; AV, azygos vein; DA, ductus arteriosus; E, esophagus; K, Kommerell diverticulum; LCA, left carotid artery; LSA, left subclavian artery; LSVC, left superior vena cava; PA, pulmonary artery; RCA, right carotid artery; RSA, right subclavian artery; RSVC, right superior vena cava; T, trachea.

the flow of the entire brachiocephalic trunk depends on a shunt from the circle of Willis.<sup>45</sup>

Multidetector computed tomography can clearly show the condition of the aortic arch, the presence or absence of the ductus, and, thus, the connection of the left subclavian artery with the pulmonary artery. It can also show the distance from the isolated vessel, whether the subclavian artery or the brachiocephalic trunk, to the aortic arch. Surgery is indicated for subclavian steal syndrome and compressive symptoms and should reconnect an isolated left subclavian artery to the left carotid artery or an isolated brachiocephalic trunk to the aortic arch.<sup>46</sup>

#### *Right Aortic Arch With Left Descending Aorta (Cervical Aortic Arch)*

In this rare malformation, the proximal and distal aortic arches are on different sides of the spine and the aorta crosses behind the trachea and esophagus<sup>9</sup> (Figure 8).

A RAA with left descending aorta (Figure 8A-D) is more frequent than a left aortic arch with right descending aorta (Figure 8E-G). For a RAA, the first vessel is the left carotid artery, whose origin is in the basal portion of the ascending aorta; the right subclavian and carotid arteries develop from the apical portion of the arch. If the arch has a supraclavicular position, it is known as a cervical aortic arch<sup>9,47</sup> (Figure 8C and D). The aortic arch connects the right ascending aorta with the left descending aorta, making a closed downward curve to direct itself toward the left of the spine, passing behind the trachea and esophagus. The left subclavian artery arises from the descending aorta to the left of the spine.<sup>9,47-49</sup> There may be a KD on the left, from which a ductal ligament can be directed toward the left pulmonary artery that closes the ring.

Patients with cervical aortic arch have a pulsatile neck mass and its compression results in a characteristic decrease in the femoral pulse.<sup>50</sup> Patients do not typically have compressive symptoms and do not usually require surgery. It has been associated with other cardiac malformations and chromosomal alterations, particularly 22q11 deletion.<sup>47-49,51</sup>

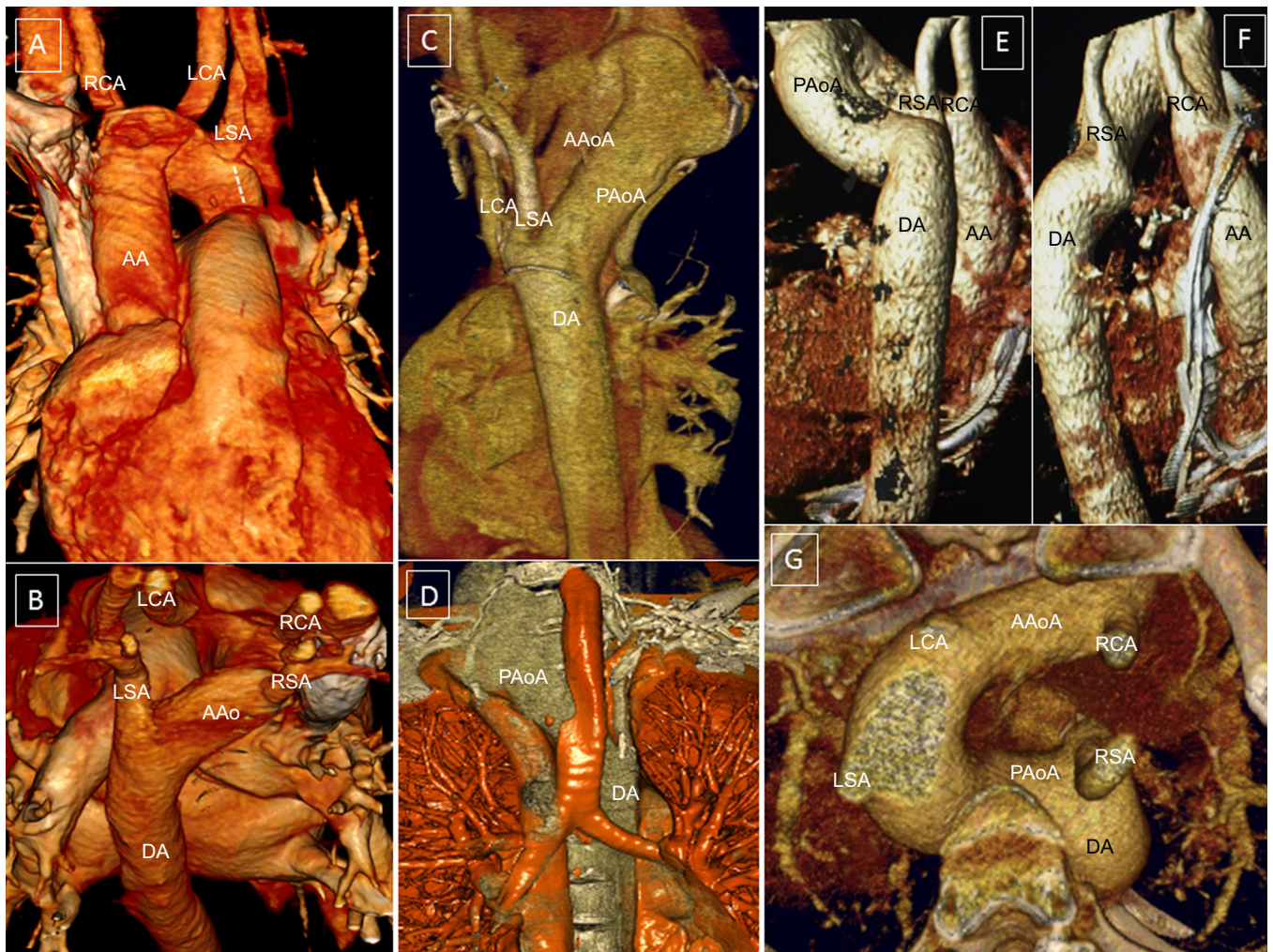


**Figure 8.** Case 1: right aortic arch with left descending aorta. A: Anterior view, 3-dimensional volumetric reconstruction; right arch and kinking of the left subclavian artery (dotted line indicating the imaginary ductal ligament). B: Posterosuperior view; the aortic arch crosses behind the trachea and esophagus. Case 2: right cervical aortic arch. C: Posterior view; superior aortic apex to the thoracic lid; deformity of the arch and the origin of the supraortic trunks at the thoracic level. D: Compression of the airway by the posterior aortic arch. Case 3: left ascending aorta with right descending aorta, aberrant right subclavian artery, and right ductal ligament; 3-dimensional volumetric reconstruction. E: Posterior view; left aortic arch crossing toward the right in front of the spine and behind the esophagus; right descending aorta. F: Right lateral view; deformity of the aortic arch due to the anchorage of the right ductal ligament in the right pulmonary artery. G: Posterosuperior view; independent origin of the 4 supraortic trunks. AA, ascending aorta; AAoA, anterior aortic arch; DA, descending aorta; LCA, left carotid artery; LSA, left subclavian artery; PAoA, posterior aortic arch; RCA, right carotid artery; RSA, right subclavian artery.

### Left Aortic Arch With Aberrant Right Subclavian Artery and Right Ductal Ligament

In these patients, the right subclavian artery develops as the last trunk at the junction of the aortic arch and the origin of the descending aorta in a KD (Figure 9A and B). The VR is formed by the ascending aorta in front, the aortic arch to the left, the aberrant subclavian artery behind, and the persistent ductus arteriosus to the right. Few cases have been reported.<sup>9</sup>

### TYPES OF VASCULAR SLINGS

#### Left Aortic Arch With Aberrant Right Subclavian Artery

The ARSA is formed in an aberrant manner as the last vessel of the arch and passes behind the esophagus and toward the right arm. A sling is formed by the ascending aorta, the aortic arch to the left, and the aberrant subclavian artery behind, without producing a complete ring. The anatomy is mirrored with respect to a RAA

with ALSA but it is not usually accompanied by a diverticulum or VR (Figure 9D).

The prevalence of ARSA in autopsy series<sup>52</sup> ranges from 1% to 2%. However, a recent fetal series has reported a much higher incidence.<sup>53</sup> In addition, it is considered a marker of Down syndrome. After various meta-analyses, the true prevalence of ARSA has been estimated to be 23.6% in Down syndrome fetuses, largely limited to those with intracardiac malformations associated with arch alterations, and 1.02% in euploid fetuses.<sup>54,55</sup>

Most patients with ARSA are asymptomatic, except those with associated intracardiac anomalies.<sup>9–11,56</sup> Isolated cases are usually detected by chance and surgery is not indicated. The condition can sometimes be symptomatic, especially in adolescents or adults.<sup>56–58</sup> Patients can have dysphagia due to esophageal compression and, when accompanied by a KD, can have aneurysmatic dilatation that produces compressive symptoms only evident in adulthood.<sup>56–58</sup> Aortic dissection and secondary aortic rupture have also been described.<sup>59</sup>

Surgery in symptomatic patients involves release of the vessel from its retroesophageal position, resection of the aneurysm, and,

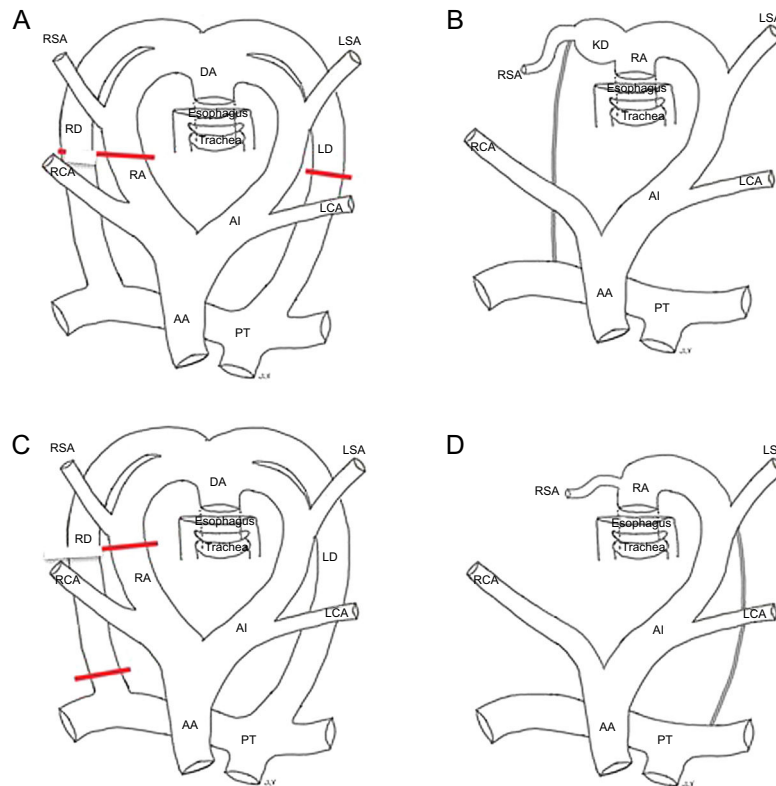


**Figure 9.** Hypothetical models and definitive diagrams. A and B: Left aortic arch with Kommerell diverticulum, aberrant subclavian artery, and right ductal ligament. C and D: Left aortic arch with aberrant right subclavian artery and left ductus (without vascular ring). AA, ascending aorta; DA, descending aorta; KD, Kommerell diverticulum; LCA, left carotid artery; LD, left ductus; LSA, left subclavian artery; PT, pulmonary trunk; RA, right arch; RCA, right carotid artery; RD, right ductus; RSA, right subclavian artery.

ideally, reestablishment of the flow from the right subclavian artery via its anastomosis with the right carotid artery. A right thoracotomy approach should be used, particularly in infants.<sup>60,61</sup> Hybrid repair techniques are also being used, such as percutaneous aortic stent placement, percutaneous diverticulum closure, and carotid artery bypass to the right subclavian artery.<sup>59,62</sup>

Multidetector computed tomography<sup>10,11,14,15,63</sup> permits the diagnosis and identification of the origin and course of the artery, the degree of compression produced, and the presence of an aortic aneurysm, these are important data for surgery and obviate the need for angiography.

### Right Aortic Arch With Aberrant Left Subclavian Artery

Right aortic arch with ALSA originating from a KD often produces a complete VR (Figures 4D and Figure 6). Less frequently, it can give rise to a vascular sling, instead of a complete ring, which would be formed by the ascending aorta in front, the aortic arch to the right, and the aberrant subclavian artery behind, so that the VR remains open. In these cases, it is not accompanied by a KD<sup>9</sup>.

### Aberrant Left Pulmonary Artery or Pulmonary Sling

In this infrequent anomaly, the left pulmonary artery originates from the proximal and posterior portion of the right pulmonary branch and is directed to the left, passing between the trachea and the esophagus, compressing both structures and forming a sling (Figure 10). For its correct diagnosis, it is essential to show not only the aberrant origin of the left pulmonary artery in the right pulmonary artery, but also its anomalous course that hugs the

trachea.<sup>9,19,63</sup> The anterior esophageal compression is a virtually pathognomonic esophagography finding for this structure.

Morena et al<sup>64</sup> were the first to discover an aberrant origin of the left pulmonary artery on the right, but with an anterior course from the trachea and esophagus without airway compression or sling formation. This entity was subsequently named a pseudosling.<sup>65</sup> The development of MDCT has permitted the discovery of cases of partial slings with a normal bifurcation of the pulmonary artery supplying one of the lobes and an anomalous origin of the artery of the other lobe in the right pulmonary artery with an aberrant course, forming a sling.<sup>66</sup>

Frequently, the pulmonary sling and airway abnormalities are associated with abnormal bronchial bifurcation patterns, secondary tracheobronchial compression, and complete cartilaginous rings (supplementary material).<sup>9,67</sup> Slings have been linked with other cardiac disorders (septal defects, persistent ductus arteriosus, tetralogy of Fallot, aortic coarctation, and persistent left superior vena cava) and extracardiac malformations.<sup>1,9,10</sup>

All affected patients require an endoscopic study of the tracheobronchial tree before surgery.<sup>63,68</sup> Both computed tomography and MRI are diagnostic, but the MDCT images and 3-dimensional reconstructions of both the sling and the airway can more accurately diagnose these anomalies.<sup>63,67</sup> Moreover, MDCT allows visualization of the airway and the vascular structures. The study time of MDCT is much shorter than that of MRI and avoids the need for general anesthesia and patient intubation, particularly important because those affected are generally infants and newborns in critical condition.

The surgical approach in sling<sup>35</sup> patients usually involves median thoracotomy with cardiopulmonary bypass, and preoperative<sup>63,67,68</sup> and intraoperative endoscopy is recommended to rule out regions of persistent malacia after the vascular surgery and

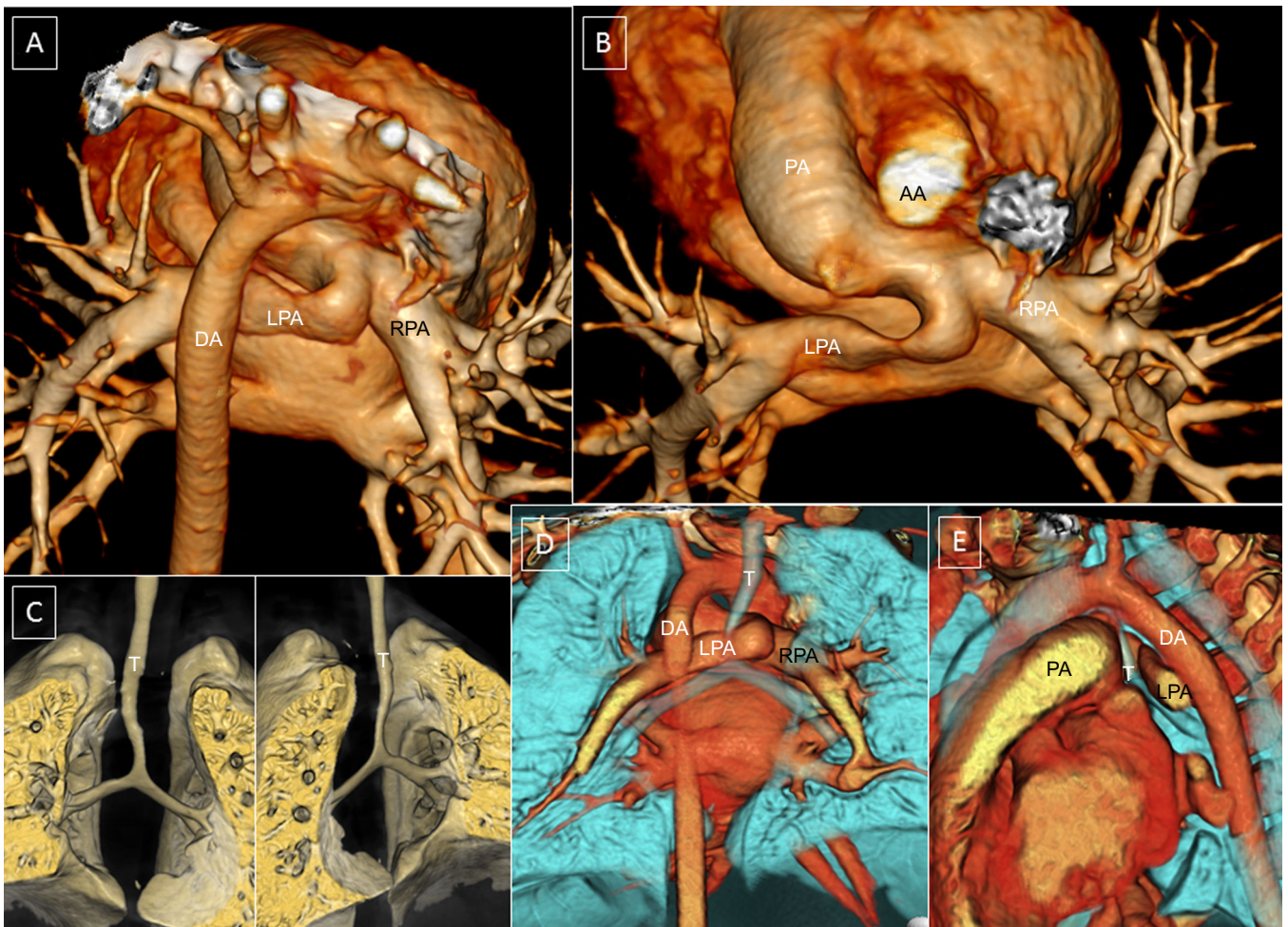


**Figure 10.** Pulmonary artery sling. Origin of the left pulmonary artery in the right pulmonary artery. A: 3-dimensional volumetric reconstruction of computed tomography coronary angiography, posterior view. B: Posterosuperior view. C: 3-dimensional reconstruction of the airway; diffuse tracheobronchial stenosis. D and E: Posterior and left lateral view of a 3-dimensional reconstruction of the vessels and airway showing all of the anatomic relationships; notice the left pulmonary artery hugging the trachea (D). AA, ascending aorta; DA, descending aorta; LPA, left pulmonary artery; PA, pulmonary artery; RPA, right pulmonary artery; T, trachea.

decide if there is a need for tracheal surgery and vessel pexy.<sup>11,15,35,36,39,68</sup>

### FINAL CONSIDERATIONS

In our experience,<sup>15,27,31,36,39,64,69</sup> low-dose MDCT with multiplanar and 3-dimensional volumetric reconstructions is the most complete technique for the study of VR. In symptomatic patients, it aids in surgical planning and can even predict the need for further tracheal surgery, which would require a multidisciplinary surgical approach. Esophagography and angiography are now rarely indicated, although their performance for other reasons may indicate the presence of previously unsuspected anomalies.

Tracheal endoscopy is frequently included in the diagnostic work-up of aortic arch anomalies. Multidetector computed tomography provides clear images of the aortic arch and any possible VR and their resultant airway compression and can often avoid the need for bronchoscopy. The latter technique can be reserved for the preoperative study of pulmonary slings, symptomatic or more complex cases, and intraoperative imaging. In those anomalies involving an ARSA or ALSA, identification is required of vascular structure dilatations compatible with KD because they would indicate a complete VR possibly requiring

surgery. Their absence, particularly in cases associated with other congenital cardiac malformations, should call into question the presence of a VR.

Currently, developments in fetal echocardiography techniques are revealing a high incidence of aortic arch malformations potentially giving rise to VR. Although many of these abnormalities are asymptomatic, it would be wise to confirm their diagnosis in the postnatal period. Given that echocardiography has little diagnostic value in aortic arch anomalies, MRI or low-dose MDCT have become the ideal techniques for this indication. Many authors recommend clinical follow and MRI only for symptomatic patients.<sup>6,17,19,43</sup> In our center, low-dose MDCT is performed to confirm or rule out suspected prenatal VR,<sup>15</sup> because this technique provides the most complete information and is the most readily available in the Spanish health care system. This imaging modality allows confirmation of the diagnosis and correct evaluation of the degree of airway involvement, as well as preventive surgical planning for asymptomatic patients but with severe involvement of the airway.

### ACKNOWLEDGMENTS

We thank Francisco Javier Lozano Vilardell from the Faculty of Fine Arts of the University of Barcelona for the drawings in [Figure 1](#), [Figure 4](#) and [Figure 9](#) and Dr. Carlos de la Torre from the Pediatric

Surgery Service, Hospital La Paz, Madrid, for the supplementary material.

## CONFLICTS OF INTEREST

None declared.

## SUPPLEMENTARY MATERIAL



Supplementary material associated with this article can be found in the online version available at doi:10.1016/j.rec.2016.03.025.

## REFERENCES

- Backer CL, Mavroudis C. Congenital heart surgery nomenclature and database project: vascular rings, tracheal stenosis, pectus excavatum. *Ann Thorac Surg.* 2000;69:5308–18.
- Gross RE. Surgical treatment for dysphagia lusoria. *Ann Surg.* 1946;124:532–4.
- Jain S, Kleiner B, Moon-Grady A, Hornberger LK. Prenatal diagnosis of vascular rings. *J Ultrasound Med.* 2010;29:287–94.
- Li S, Luo G, Norwitz ER, Wang C, Ouyang S, Yao Y, et al. Prenatal diagnosis of congenital vascular rings and slings: sonographic features and perinatal outcome in 81 consecutive cases. *Prenat Diagn.* 2011;31:334–46.
- Tuo G, Volpe P, Bava GGL, Bondanza S, de Robertis V, Pongiglioni G, et al. Prenatal diagnosis and outcome of isolated vascular rings. *Am J Cardiol.* 2009;103:416–9.
- Galindo A, Nieto O, Nieto MT, Rodríguez-Martín MO, Herraiz I, Escibano D, et al. Prenatal diagnosis of right aortic arch: associated findings, pregnancy outcome, and clinical significance of vascular rings. *Prenat Diagn.* 2009;29:975–81.
- Bjornard K, Riehle-Colarusso T, Gilboa SM, Correa A. Patterns in the prevalence of congenital heart defects, metropolitan Atlanta, 1978 to 2005. *Birth Defects Res A Clin Mol Teratol.* 2013;97:87–94.
- Ferencz C. Epidemiology of congenital heart disease: The Baltimore-Washington infant study 1981–1989. In: Ferencz C, Rubin JD, Ioffredo CA, Magee CA, editors. *Perspectives in pediatric cardiology.* Vol. 4. Mount Kisco: Futura; 1993.
- Yoo SH, Bradley TJ. Vascular rings, pulmonary arterial sling, and related conditions, chapter 47. In: Anderson RH, Baker EJ, Penny DJ, Redington AN, Rigby ML, Wernovsky G, editors. *Paediatric cardiology.* 3rd ed. Philadelphia: Churchill Livingstone; 2010. p. 967–89.
- Berdon WE. In: Gross EMD, Edward BD, editors. *Rings slings and other things: vascular compression of the infant trachea updated from the midcentury to the millennium—the legacy of Robert, 216.* Neuhauser, MD: Radiology; 2000. p. 624–32.
- Dodge-Khatami A, Tulevski II, Hitchcock JF, de Mol BA, Bennink GB. Vascular rings and pulmonary arterial sling: From respiratory collapse to surgical cure, with emphasis on judicious imaging in the hi-tech era. *Cardiol Young.* 2002;12:96–104.
- Berg C, Bender F, Soukup M, Geipel A, Axt-Flidner R, Breuer J, et al. Right aortic arch detected in fetal life. *Ultrasound Obstet Gynecol.* 2006;28:882–9.
- Kohl G. The evolution and state-of-the-art principles of multislice computed tomography. *Proc Am Thorac Soc.* 2005;2:470–500.
- Etesami M, Ashwath R, Kanne J, Gilkeson RC, Rajiah P. Computed tomography in the evaluation of vascular rings and slings. *Insights Imaging.* 2014;5:507–21.
- Bret-Zurita M, Cuesta E, Cartón A, Díez J, Aroca A, Oliver JM, et al. Utilidad de la tomografía computarizada de 64 detectores en el diagnóstico y el manejo de los pacientes con cardiopatías congénitas. *Rev Esp Cardiol.* 2014;67:898–905.
- Yagel S, Arbel R, Anteby EY, Raveh D, Achiron R. The three vessels and trachea view (3VT) in fetal cardiac scanning. *Ultrasound Obstet Gynecol.* 2002;20:340–5.
- Razon Y, Berant M, Fogelman R, Amir G, Birk E. Prenatal diagnosis and outcome of right aortic arch without significant intracardiac anomaly. *J Am Soc Echocardiogr.* 2014;27:1352–8.
- Kanne JP, Godwin JD. Right aortic arch and its variants. *J Cardiovasc Comput Tomogr.* 2010;4:293–300.
- D'Antonio F, Khalil A, Zidere V, Carvalho JS. Fetuses with right aortic arch multicentre cohort study and meta-analysis. *Ultrasound Obstet Gynecol.* 2016;47:423–32.
- Frush DP, Herlong JR. Pediatric thoracic CT angiography. *Pediatr Radiol.* 2005;35:11–25.
- Efstathopoulos EP, Kelekis NL, Pantos I, Brountzos E, Argentos S, Grebac J, et al. Reduction of the estimated radiation dose and associated patient risk with prospective ECG-gated 256-slice CT coronary angiography. *Phys Med Biol.* 2009;54:5209–22.
- Hollingsworth CL, Yoshizumi TT, Frush DP, Chan FP, Toncheva G, Nguyen G, et al. Pediatric cardiac-gated CT angiography: assessment of radiation dose. *AJR Am J Roentgenol.* 2007;189:12–8.
- Callahan MJ, Poznauskis L, Zurakowski D, Taylor GA. Nonionic iodinated intravenous contrast material-related reactions: incidence in large urban children's hospital-retrospective analysis of data in 12,494 patients. *Radiology.* 2009;250:674–81.
- Congdon ED. Transformation of the aortic-arch system during the development of the human embryo. *Contrib Embryol.* 1922;14:47–110.
- Edwards JE. Anomalies of the derivatives of the aortic arch system. *Med Clin North Am.* 1948;32:925–48.
- McElhinney DB, Hoydu AK, Gaynor JW, Spray TL, Goldmuntz E, Weinberg PM. Patterns of right aortic arch and mirror-image branching of the brachiocephalic vessels without associated anomalies. *Pediatr Cardiol.* 2001;22:285–9.
- Núñez-Gil IJ, García-Guereta L, Bret-Zurita M. Real vision of a vascular ring. *Eur Heart J Cardiovasc Imaging.* 2012;13:279.
- Afzal MN. Fatal double aortic arch anomaly and maternal cocaine abuse. *J Coll Physicians Surg Pak.* 2003;13:166–7.
- Knight L, Edwards JE. Right aortic arch. Types and associated cardiac anomalies. *Circulation.* 1974;50:1047–51.
- Kömmerell B. Verlagerung des Ösophagus durch eine abnorm verlaufende Arteria subclavia dextra (Arteria lusoria). *Dtschsch Geb Roentgenstrahlen.* 1936;54:590–5.
- Deiros-Bronte L, Rodríguez R, Centeno F, Ferrer Q, Galindo A, García de la Calzada D, et al. Prenatal diagnosis of right aortic arch: A Spanish multicenter study. *Cardiol Young.* 2013;23 Suppl 1:S15.
- Cina CS, Althani MDH, Pasenau J, Abouzahr L. Kömmerell's diverticulum and right-sided aortic arch: A cohort study and review of the literature. *J Vasc Surg.* 2004;39:131–9.
- Floten HS, Rose DM, Cunningham JN Jr. Surgical therapy of a dissecting aortic aneurysm involving a right-sided aortic. *J Am Coll Cardiol.* 1984;4:1058–61.
- Dikman SH, Baron M, Gordon AJ. Right aortic arch with ruptured aneurysm of anomalous left subclavian artery. *Am J Cardiol.* 1974;34:245–9.
- Kouchoukos N, Blackstone E, Doty D, Hanley F, Karp R. Vascular ring and sling. In: Kouchoukos NT, Blackstone EH, Hanley FL, Kirklin JK, editors. *Kirklin/Barratt-Boyes cardiac surgery.* 3<sup>rd</sup> ed. Oxford: Churchill Livingstone; 2003. p. 1415–26.
- Cordovilla Zurdo G, Cabo Salvador J, Sanz Galeote E, Moreno Granados F, Alvarez Diaz F. Vascular rings of aortic origin: the surgical experience in 43 cases. *Rev Esp Cardiol.* 1994;47:468–75.
- Burke RP, Rosentfeld HM, Wernovsky G, Jonas RA. Video-assisted thoracoscopic vascular ring division in infants and children. *J Am Coll Cardiol.* 1995;25:943–7.
- Kogon BE, Forbess JM, Wulkan ML, Kirshbom PM, Kanter KR. Video-assisted thoracoscopic surgery: is it a superior technique for the division of vascular rings in children? *Congenit Heart Dis.* 2007;2:130–3.
- Sánchez Pérez R, Rey J, Polo López L, Aroca Peinado A, González Rocafort A, Pérez González R, et al. Anillos vasculares y compresión traqueo-esofágica: 15 años de experiencia quirúrgica. *Cir Cardiovas.* 2016;23:119–24.
- Backer CL, Russell HM, Wurlitzer KC, Rastatter JC, Rigby CK. Primary resection of Kömmerell diverticulum and left subclavian artery transfer. *Ann Thorac Surg.* 2012;94:1612–7.
- Luciano D, Mitchell J, Fraise A, Lepidi H, Kreitmann B, Ovaert C. Kömmerell diverticulum should be removed in children with vascular ring and aberrant left subclavian artery. *Ann Thorac Surg.* 2015;100:2293–7.
- Backer CL, Mongé MC, Russell HM, Popescu AR, Rastatter JC, Costello JM. Reoperation after vascular ring repair. *Semin Thorac Cardiovasc Surg Pediatr Card Surg Ann.* 2014;17:48–55.
- Miranda JO, Callaghan N, Miller O, Simpson J, Sharland G. Right aortic arch diagnosed antenatally: associations and outcome in 98 fetuses. *Heart.* 2014;100:54–9.
- Männer J, Seidl W, Steding G. The formal pathogenesis of isolated common carotid or innominate arteries: the concept of malseptation of the aortic sac. *Anat Embryol.* 1997;196:435–45.
- Reeves BM, Colen TM, Sheridan BJ, Ward C. Isolated innominate artery as a cause of subclavian steal and cerebral hemisphere atrophy. *Pediatr Cardiol.* 2010;31:1083–5.
- Gil-Jaurena JM, Ferreiros M, Zabala I, Cuenca V. Right aortic arch with isolation of the left innominate artery arising from the pulmonary artery and atrial septal defect. *Ann Thorac Surg.* 2011;91:303.
- Baravelli M, Borghi A, Rogiani S, Preda L, Quattrocchi M, Fantoni C, et al. Clinical, anatomopathological and genetic pattern of 10 patients with cervical aortic arch. *Int J Cardiol.* 2007;114:236–40.
- Sobrinho Márquez JM, Gozalves I, Gómez A, Fernández A, Santos J, Descalzo A. Arco aórtico cervical asociado a cardiopatía. *Rev Esp Cardiol.* 1992;45:537–40.
- Vázquez C, Cabrera A, Oñate A, Pastor E. Arco aórtico cervical tipo A: Descripción de un caso asociado a tetralogía de Fallot y estenosis de rama pulmonar. *Rev Esp Cardiol.* 1983;36:265–8.
- Mullins CE, Gillette PC, McNamara DG. The complex of cervical aortic arch. *Pediatrics.* 1973;51:210–5.
- McElhinney DB, Clark BJ, Weinberg PM, Kenton ML, McDonald-McGinn D, Driscoll DA, et al. Association of chromosome 22q11 deletion with isolated anomalies of aortic arch laterality and branching. *J Am Coll Cardiol.* 2001;37:2114–9.
- Zapata H, Edwards JE, Titus JL. Aberrant right subclavian artery with left aortic arch: associated cardiac anomalies. *Pediatr Cardiol.* 1993;14:159–61.
- Chaoui R, Heling KS, Sarioglu N, Schwabe M, Dankof A, Bollmann R. Aberrant right subclavian artery as a new cardiac sign in second- and third-trimester fetuses with Down syndrome. *Am J Obstet Gynecol.* 2005;192:257–63.

54. Scala C, Leone Roberti Maggiore U, Candiani M, Venturini PL, Ferrero S, Greco T, et al. Aberrant right subclavian artery in fetuses with Down syndrome: a systematic review and meta-analysis. *Ultrasound Obstet Gynecol.* 2015;46:266–76.
55. de León-luis J, Gámez F, Bravo C, Tenías JM, Arias Á, Pérez R, et al. Second-trimester fetal aberrant right subclavian artery: original study, systematic review and meta-analysis of performance in detection of Down syndrome. *Ultrasound Obstet Gynecol.* 2014;44:147–53.
56. Grathwohl KW, Afifi AY, Dillard TA, Olson JP, Heric BR. Vascular rings of the thoracic aorta in adults. *Am Surg.* 1999;65:1077–83.
57. de Araújo G, Junqueira Bizzi JW, Muller J, Cavazzola LT. “Dysphagia lusoria” – Right subclavian retroesophageal artery causing intermittent esophageal compression and eventual dysphagia—A case report and literature review. *Int J Surg Case Rep.* 2015;10:32–4.
58. Guzman ED, Eagleton MJ. Aortic dissection in the presence of an aberrant right subclavian artery. *Ann Vasc Surg.* 2012;26:860. e13-8.
59. Wong RH, Chow SC, Lok JK, Nq CS, Yu SC, Lau JY, et al. Hybrid treatment for ruptured diverticulum of Kömmerell: a minimally invasive option. *Ann Thorac Surg.* 2013;95:e95–6.
60. Atay Y, Engin C, Posacioglu H, Ozyurek R, Ozcan C, Yagdi T, et al. Surgical approaches to the aberrant right subclavian artery. *Tex Heart Inst J.* 2006;33:477–81.
61. Kieffer E, Bahnini A, Koskas F. Aberrant subclavian artery: surgical treatment in thirty-three adult patients. *J Vasc Surg.* 1994;19:100–9.
62. van Bogerijen GH, Patel HJ, Eliason JL, Criado E, Williams DM, Knepper J, et al. Evolution in the management of aberrant subclavian arteries and related Kommerell diverticulum. *Ann Thorac Surg.* 2015;100:47–53.
63. Leonardi B, Secinaro A, Cutrera R, Albanese S, Trozzi M, Franceschini A, et al. Imaging modalities in children with vascular ring and pulmonary artery sling. *Pediatr Pulmonol.* 2015;50:781–8.
64. Moreno F, Garcia-Guereta L, Benito F, Gamallo C, Campo F, Herranz F, et al. Aberrant left pulmonary artery with tracheal stenosis without vascular sling. *Pediatr Cardiol.* 1991;12:44–5.
65. Jan SL, Tsai IC, Ho CL, Lin MC, Fu YC. Pseudopulmonary artery sling in a 22q11 deletion newborn with tetralogy of Fallot and isolated left subclavian artery. *Echocardiography.* 2008;25:931–3.
66. Collell R, Marimón C, Montero M. Partial left pulmonary artery sling. *Rev Esp Cardiol.* 2010;63:850.
67. Heyer CM, Nuesslein TG, Jung D, Peters SA, Lemburg SP, Rieger CH, et al. Tracheobronchial anomalies and stenoses: detection with low-dose multidetector CT with virtual tracheobronchoscopy-comparison with flexible tracheobronchoscopy. *Radiology.* 2007;242:542–9.
68. Hazekamp MG, Koolbergen DR, Kersten J, Peper J, de Mol B, König-Jung A. Pediatric tracheal reconstruction with pericardial patch and strips of autologous cartilage. *Eur J Cardiothorac Surg.* 2009;36:344–51.
69. Cartón AJ, González Á, Bret Zurita M. Coartación del lado equivocado del arco aórtico. *Rev Esp Cardiol.* 2013;66:497.